Aerosol Science and Technology

ISSN: 0278-6826 (Print) 1521-7388 (Online) Journal homepage: http://www.tandfonline.com/loi/uast20

Performance Evaluation and Use of a Continuous Monitor for Measuring Size-Fractionated PM 2.5 Nitrate

Philip M. Fine , Peter A. Jaques , Susanne V. Hering & Constantinos Sioutas

To cite this article: Philip M. Fine , Peter A. Jaques , Susanne V. Hering & Constantinos Sioutas (2003) Performance Evaluation and Use of a Continuous Monitor for Measuring Size-Fractionated PM 2.5 Nitrate, Aerosol Science and Technology, 37:4, 342-354, DOI: 10.1080/02786820300964

To link to this article: http://dx.doi.org/10.1080/02786820300964

Published online: 30 Nov 2010.

Submit your article to this journal

Article views: 127

View related articles

Citing articles: 6 View citing articles

Full Terms & Conditions of access and use can be found at
http://www.tandfonline.com/action/journalInformation?journalCode=uast20

Download by: [University of North Texas] **Date:** 06 January 2017, At: 21:47

Aerosol Science and Technology 37: 342–354 (2003)
© 2003 American Association for Aerosol Research
Published by Taylor and Francis
0278-6826/03/$12.00 + .00
DOI: 10.1080/02786820390125188

Performance Evaluation and Use of a Continuous Monitor for Measuring Size-Fractionated $PM_{2.5}$ Nitrate

Philip M. Fine,[1] Peter A. Jaques,[2] Susanne V. Hering,[3] and Constantinos Sioutas[1]
[1]*Department of Civil and Environmental Engineering, University of Southern California, Los Angeles, California*
[2]*School of Public Health, University of California at Los Angeles, Los Angeles, California*
[3]*Aerosol Dynamics Inc., Berkeley, California*

A field evaluation of a new size-fractionating continuous fine particle nitrate monitor from Aerosol Dynamics Inc. (ADI), Berkeley, CA was conducted via comparison to traditional time-integrated filter (HEADS) and impactor (MOUDI) measurements. The new monitor consists of three cascaded integrated collection and vaporization cells (ICVC) and provides 10-min resolution particulate nitrate measurements in three particle diameter size ranges (0.10–0.45, 0.45–1.0, and 1.0–2.5 μm) corresponding to observed submodes in the particle size distribution in Southern California. Side-by-side sampling was conducted for approximately six months at two sites, both at downwind receptor locations east of downtown Los Angeles. Both size-resolved and total $PM_{2.5}$ nitrate concentrations were compared among the different sampling techniques. The ADI monitor and HEADS $PM_{2.5}$ nitrate measurements, for which nitrate sampling artifacts are expected to be low, are well correlated ($r^2 = 0.79$) with a geometric mean ADI:HEADS ratio of 0.90. The ADI size-fractionated nitrate data measured consistently more nitrate than the corresponding MOUDI stages due to volatilization of labile ammonium nitrate from the MOUDI impaction substrates. Less disagreement was observed in the 1.0–2.5 μm size range in which nitrate is more likely to exist as nonlabile sodium nitrate. The observed MOUDI nitrate losses are attributable to existing theories of nitrate sampling efficiencies and losses. The continuous nature of the data generated by the ADI monitor will provide valuable information on the spatial and temporal distribution of particulate nitrate in the atmosphere, and the new dimension of size-fractionation can help to determine the sources and formation mechanisms of atmospheric particulate nitrate as well. Examples of the atmospheric data generated in this study are presented and the potential utility of such data provided by the new monitor are discussed.

Received 8 May 2002; accepted 1 October 2002.
This work was supported in part by the Southern California Particle Center and Supersite (SCPCS), funded by the U.S. EPA under the STAR program. Although the research described in this article has been funded in part by the United States Environmental Protection Agency through grants # 53-4507-0482 and 53-4507-7721 to USC, it has not been subjected to the Agency's required peer and policy review and therefore does not necessarily reflect the views of the Agency, and no official endorsement should be inferred.
Address correspondence to Constantinos Sioutas, Department of Civil and Environmental Engineering, University of Southern California, 3620 South Vermont Avenue, Loss Angeles, CA 90089. E-mail: sioutas@usc.edu

INTRODUCTION

Ambient particulate matter (PM) has been the primary focus of several epidemiological studies, which indicated a strong correlation between adverse respiratory effects and particle concentration levels (Dockery et al. 1993; Gordian et al. 1996; Schwartz and Dockery 1992). Most of the health effects have been associated with the ambient mass concentration of particles smaller than 10 μm or, more recently, 2.5 μm in aerodynamic diameter. Nevertheless, fundamental uncertainty and disagreement persist regarding which physical and chemical properties of atmospheric particles (or unidentified confounding environmental influences) can influence health risks, what pathophysiological mechanisms are operative, and which air quality regulations should be adopted to reduce the risk to human health (Vedal 1997). Since the numerous chemical constituents of particulate matter have varying degrees of toxicity, accurate determination of the chemical composition of PM is essential in assessing its health effects on humans.

The most commonly used techniques for separating particles from ambient gases are time-integrated particle collection methods such as filtration and/or impaction. The sampling time periods for such methods typically range from 4 to 48 h in order to collect sufficient sample for analysis. Important parameters that will affect PM composition include the temperature, the relative humidity (RH), the emission strength of various sources, the mixing depth of the atmosphere, and the atmospheric concentrations of gaseous precursors. Since all of these factors can vary substantially over the course of a day, short sampling time scales are essential in developing a better understanding of PM

sources and formation mechanisms. Furthermore, a number of labile particulate species are difficult to sample because of physical or chemical changes that may occur during or after prolonged sample collection. Particulate ammonium nitrate and organic carbon are the two predominant labile PM species and are also two of the most abundant constituents of particles in urban areas such as the Los Angeles Basin (Christoforou et al. 2000). Time-integrated sampling of labile species often leads to errors (artifacts), resulting in an underestimation or overestimation of the particulate phase (Appel et al. 1984; Coutant 1977; Hering and Cass 1999). There are denuder and filter-based methods available which can correct for such sampling artifacts. However, they are not currently being used in most sampling networks and do require additional resources.

Evidence of negative artifacts in particulate nitrate measurements has been discussed extensively in the literature (Appel and Tokiwa 1983; Appel et al. 1984; Eatough et al. 1988; Smith et al. 1978; Wang and John 1988; Witz et al. 1990). Losses of ammonium nitrate during sampling have been attributed to either an increase in pressure drop across the particle-collecting medium or to changes in the solid-gas equilibrium between particulate ammonium nitrate and gas-phase nitric acid and ammonia during sampling. Nitrate losses due to changes in the solid-gas phase equilibrium are due to the dependence of the dissociation constant of ammonium nitrate on temperature and RH, and it is generally accepted that at high temperature or low humidity, this dissociation constant will increase (Forrest et al. 1980; Mozurkewich 1993; Stelson and Seinfeld 1982; Wexler and Seinfeld 1991). Ammonium nitrate is a major fine particle component in Southern California, and the evaporative losses under common high temperature and low RH conditions can significantly affect measurements of fine particle nitrate and mass.

In order to obtain fine particle nitrate measurements on shorter time scales and reduce nitrate sampling errors associated with time-integrated sampling, an automated collection and analysis method for high-time resolution determination of the major chemical constituents of ambient particles has been developed and tested (ADI integrated collection and vaporization cell (ICVC)) (Stolzenburg and Hering 2000). Comparisons between this monitor and several different filter-based nitrate sampling methods showed very good agreement ($0.94 < R^2 < 1.00$, regression slopes between 0.96 and 1.06). This previously described method has been improved to provide 10-minute nitrate measurements in three distinct particle size ranges. This article describes the field evaluation and some results of the new nitrate monitor, while a companion article presents results from the laboratory characterization of the monitor's response to generated aerosols of known size and composition (Stolzenburg et al. 2002).

The field evaluation of the new nitrate monitor was performed via a comparison to parallel time-integrated size-resolved nitrate measurements from a micro-orifice uniform-deposit impactor (MOUDI) and fine particle nitrate measurements from a Harvard EPA annular denuder system (HEADS). Correlations between the instruments will serve to validate the new monitor's field performance, while some systematic differences are attributable to anticipated nitrate losses. In addition, some examples of the atmospheric data provided by the new monitor will demonstrate its utility in helping to determine the sources and formation mechanisms of particulate nitrate in the Southern California airshed.

METHODS

Description of the Size-Segregated Integrated Collection and Vaporization Cell for Continuous Nitrate Measurements

The ADI cascaded ICVC is an automated collection and analysis method for high-time resolution determination of the major chemical constituents of ambient particles. The sampler is an extension of a previously developed continuous nitrate monitor (Stolzenburg and Hering 2000), which provides 10-min automated measurement of nitrate. The cascaded system enables near-continuous nitrate measurements in three size ranges of $PM_{2.5}$: 0.10–0.45, 0.45–1.0, and 1.0–2.5 μm. The choice of these three size cuts is based on previous studies over the past 10 years in Southern California (Hering et al. 1997; John et al. 1990) which have indicated that the accumulation mode may consist of two submodes, one peaking at around 0.2–0.3 μm and the other at about 0.6–0.7 μm. The first mode is created by gas-to-particle condensation of pollutant species and their atmospheric reaction products, whereas the second mode results from hygroscopic growth of sulfates and nitrates.

The design and laboratory evaluation of the size-segregated ADI continuous nitrate monitor is described in detail by Stolzenburg et al. (2002) and a schematic of the instrument can be found in that article. Thus, only a brief description will be presented in this article. The monitor consists of a preimpactor, a multicell denuder, a humidification system that brings the RH of the sampled aerosols to 65%, followed by three cascaded ICVC cells, each of which is preceded by a impaction stage. The preimpactor excludes particles above 2.5 μm. The denuder is an activated carbon-impregnated ceramic honeycomb manufactured by Corning, Toms River, NJ. The humidifier is a 300 mm long, 2.2 mm i.d. tube of Nafion surrounded by a jacket of water (Perma Pure MH110). RH is controlled to a near-constant level by means of a feedback system that controls the absolute pressure of saturated vapor in the annular region of the Nafion dryer. Humidification is needed to wet the particles so that they adhere upon impaction. The 65% RH is above the deliquescence point of ammonium nitrate and is chosen to ensure that ambient particles are wet while not leading to excessive growth. For a dry, pure ammonium nitrate particle, the diameter growth factor at 65% RH is 1.3 (Tang 1980), but the humidification also reduces the particle density, and thus the aerodynamic diameter grows by only 14%.

Following humidification, particles enter a cascade of three ICVC cells. In each cell, they are collected by impaction onto a small area (approximately 1 mm in diameter) on a solid substrate,

and then assayed in place by rapid heating of the substrate in a nitrogen atmosphere and subsequent analysis of the evolved vapors. The evolved vapors are quantified with a chemiluminscent nitrogen oxide analyzer operated with a molybdenum catalyst that reduces higher nitrogen oxides to nitric oxide. The analysis step is just under 2 min. Typical collection periods are 8 min, resulting in an overall cycle time of 10 min.

Field Experiments

For its field characterization, the cascaded ICVC system operated inside a mobile particle laboratory developed by the Southern California Particle Center and Supersite (SCPCS) measurement and monitoring program, funded by the U.S. EPA. During the period of this study, measurements were conducted at two sites for about six months and across separate seasons. From July 13 through September 15, 2001, sampling was done in Rubidoux, and from September 15, 2001 through February 10, 2002, sampling was performed in Claremont, CA. Both Rubidoux and Claremont are receptor areas of the eastern inland valleys of the basin, in which the aerosol plume generated by the millions of vehicles, mostly west of downtown Los Angeles, is advected by the predominant westerly winds after aging for several hours to a day (Pandis et al. 1992). Rubidoux (unlike Claremont) also lies downwind of significant ammonia emissions from nearby farming and livestock areas, which results in high concentrations of ammonium nitrate (Christoforou et al. 2000). Size-segregated $PM_{2.5}$ nitrate concentration measurements made by the ADI ICVC were compared to those measured with a colocated MOUDI™ impactor (MSP Corp. Minneapolis, MN) and a HEADS sampler (Koutrakis et al. 1992). MOUDI and HEADS sampled approximately once per week and for time periods varying from 4 to 24 h, depending on location and observed pollution levels. Particles were classified by the MOUDI in the following aerodynamic particle diameter ranges: <0.10, 0.10–0.32, 0.32–0.56, 0.56–1.0, and 1.0–2.5 μm. Teflon filters with diameters of 4.7 and 3.7 cm (2 μm pore size, Gelman Science, Ann Arbor, MI) were used to collect particles in the MOUDI stages and after-filter, respectively. The MOUDI does not have a 0.45 μm cut-point stage. Therefore, in order to make the MOUDI cutoff size ranges correspond to those of the ADI ICVC monitor, half of the nitrate mass determined in the 0.32–0.56 μm size range was added to that measured in the 0.10–0.32 μm range and half to that in the 0.56–1.0 μm range. This division was justified as follows: assuming that the generated nitrate particles are log normally distributed (an assumption corroborated by data obtained concurrently with other monitors as part of the Supersite program), about 50% of the particle mass in the 0.32–0.56 μm size range should be found above and below the geometric mean of that range, which is equal to 0.43 μm. This division is virtually identical to the 0.45 μm cut-point of the ADI ICVC monitor. The introduced uncertainty is minimal given the narrow width of this particle size range.

The HEADS used a carbonate-coated glass denuder to remove nitric acid, followed by a Teflon filter and two sodium carbonate filters to collect particle nitrate and to correct for positive artifacts from nitrogen dioxide. It was thus used as a reference sampler to yield, presumably, the total artifact-free $PM_{2.5}$-bound particulate nitrate.

Comparisons between the time-integrated measurements and the ADI monitor were made by averaging the continuous nitrate data across the corresponding time period of the filter and impactor samples. The size-segregated measurements of the ADI monitor and the MOUDI were combined to yield total $PM_{2.5}$data for comparison to the HEADS $PM_{2.5}$ samples.

The Teflon filters of both MOUDI and HEADS samplers were pre- and postweighed using a Mettler Microbalance (MT5, Mettler-Toledo, Inc, Hightstown, NJ) after 24-h equilibration under controlled humidity (35–40%) and temperature (22–24 °C) to determine particle mass concentrations (which are not reported here). Subsequently, the Teflon and glass fiber filters were extracted with a mixture of 5 mL of ultrapure deionized water and 0.15 mL ethanol and analyzed via ion chromatography to measure the concentration of nitrate. The equivalence of the two nitrate analysis techniques used for the current comparison (chemiluminescence nitrogen oxide analysis for the ADI monitor and ion chromatography for the filters and MOUDI substrates) was demonstrated with the nonsize-selective ADI nitrate monitor (Stolzenburg and Hering 2000).

RESULTS AND DISCUSSION

Field Comparison with MOUDI and HEADS

Results from the field intercomparison between the size-fractionated and $PM_{2.5}$ nitrate concentrations measured by the ADI monitor, the MOUDI, and the HEADS are shown in Figures 1 and 2 and summarized in Table 1. The MOUDI sampler is expected to be subject to greater sampling losses of ammonium nitrate than the HEADS sampler, which is designed to minimize nitrate sampling artifacts. Figure 1a confirms this outcome, showing that while well correlated ($r^2 = 0.88$), the HEADS sampler measures nitrate at consistently higher levels than the sum of the three MOUDI stages. As seen in Table 1, the geometric mean of the ratios of the MOUDI to the HEADS measurements is 0.57 with a very low p-value ($p < 0.01$), indicating a significant difference from a ratio of 1. The better agreement between MOUDI and HEADS for sulfate, a nonvolatile species shown in Figure 1b, indicates that the difference in nitrate measurements may be due to volatilization from the MOUDI stages and not due to errors in flow rate measurements or other systematic differences in the sampling techniques. The slope in Figure 1b of 0.85 is highly influenced by three or four outlying points, with most of the other data lying very close to the 1:1 line.

Figure 1c compares the nitrate measured by the sum of the ADI monitor size fractions, averaged over the appropriate time interval, to the nitrate measured by the HEADS sampler. The measurements are well correlated ($r^2 = 0.79$), the ADI monitor measuring slightly less nitrate than the HEADS with a

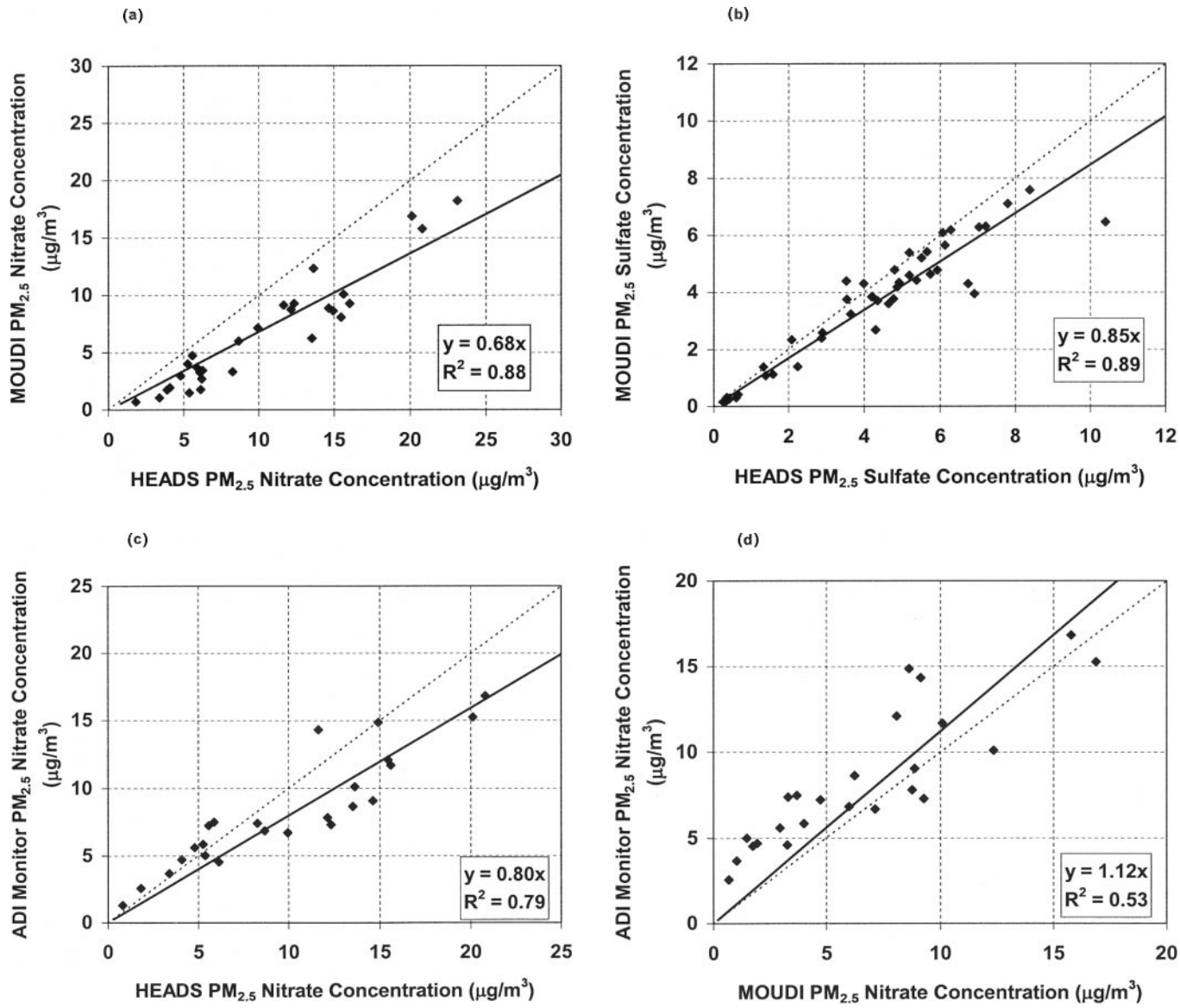

Figure 1. (a) Plot of HEADS $PM_{2.5}$ vs. summed MOUDI stages nitrate concentrations, (b) plot of HEADS $PM_{2.5}$ vs. summed MOUDI stage sulfate concentrations, (c) plot of summed ADI monitor stages vs. HEADS $PM_{2.5}$ nitrate concentrations, and (d) plot of summed ADI monitor stages vs. summed MOUDI stages nitrate concentrations.

geometric mean of the ratios between measurements of 0.90. A close inspection of Figure 1c reveals that at lower atmospheric nitrate concentrations, the ADI monitor compares well with the HEADS sampler, and the at higher nitrate concentrations, the HEADS sampler generally measures more nitrate than the ADI. The lower nitrate concentrations were mostly seen during the fall and winter months at Claremont when 24-h samples were collected. Higher nitrate concentrations occurred in the summer diurnal sampling (4, 6, or 10 h) at Rubidoux. Particulate ammonium nitrate concentrations in Rubidoux are very high in the summer due to the known upwind ammonia source at the dairy farms in Chino. Thus differences at Rubidoux may be due to increased ammonium nitrate volatilization from the ADI stages when ammonium nitrate concentrations are very high. Because of the short 10-min sampling time and the humidification process in the ADI monitor, nitrate volatilization losses should, in general, be relatively low and compare more favorably to the HEADS measurements than the MOUDI measurements described below. The slightly lower ADI values may also be explained by some nitrate associated with particles below 0.1 μm in diameter, which escape collection on the final ADI stage, or by possible internal particle losses in the ADI monitor inlet tubing. Note that the difference between the ADI and the HEADS is not statistically different from 1 ($p = 0.25$).

Table 1
Summary of comparison between the ADI monitor, MOUDI, and HEADS nitrate concentrations

Instruments compared	Particle size range (μm)	Geometric mean of the ratios	Mean difference $\pm$SD [mean relative difference]	p Value
MOUDI:HEADS	$PM_{2.5}$	0.57* (n = 29)	-3.49 ± 1.9 [-34%]	0.01
ADI:HEADS	$PM_{2.5}$	0.90 (n = 25)	-1.59 ± 2.5 [-16%]	0.25
ADI:MOUDI	1.0–2.5	1.26 (n = 21)	0.37 ± 0.6 [14%]	0.19
ADI:MOUDI	0.45–1.0	1.43* (n = 21)	0.92 ± 1.6 [27%]	0.05
ADI:MOUDI	0.10–0.45	1.33 (n = 19)	0.53 ± 0.8 [18%]	0.14

*Indicates significantly different value than 1 at the $p = 0.05$ level.

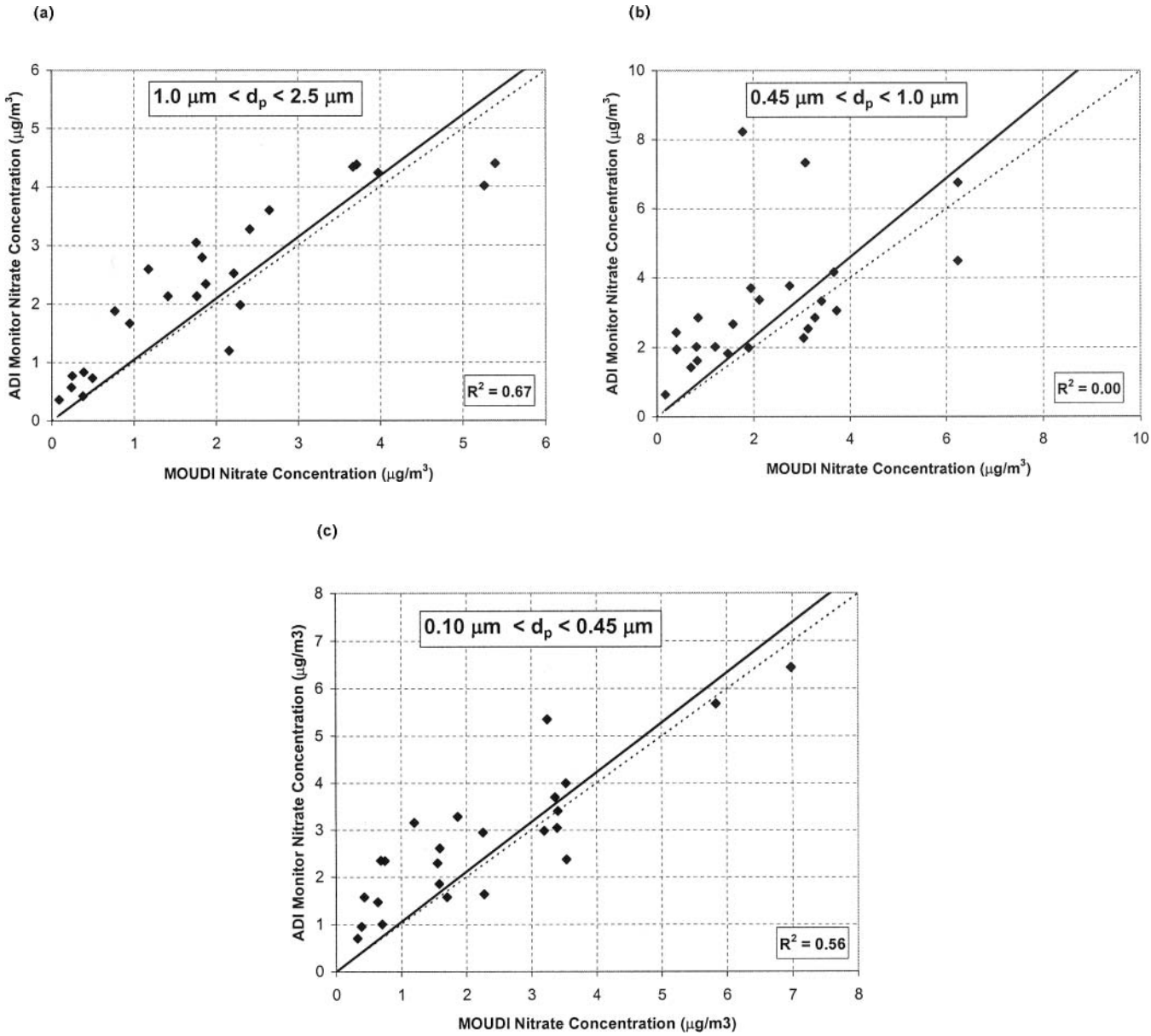

Figure 2. Comparison of size-resolved nitrate measurements by the ADI monitor and the MOUDI for particle diameters in the range (a) 1.0–2.5 μm, (b) 0.45–1.0 μm, and (c) 0.10–0.45 μm.

The total $PM_{2.5}$ ADI monitor and MOUDI nitrate measurements are compared in Figure 1d. Due to the previously discussed nitrate sampling losses in the MOUDI, the ADI monitor data is generally higher than the MOUDI, with most data points lying above the one-to-one line. The correlation in this case is lower ($r^2 = 0.53$), most likely due to varying degrees of nitrate loss on the MOUDI stages with differing temperature and humidity conditions (see discussion of theoretical nitrate losses below).

Figures 2a–c compare the size-fractionated nitrate measurements of the ADI monitor and the MOUDI. The poor correlation for the middle size fraction (0.45–1.0 μm) is due to two outlying data points, which were included in the regression calculation for the purposes of completeness but are as yet unexplained (excluding the two outliers increases the correlation coefficient to $r^2 = 0.73$). Higher ADI concentrations measured in the 0.45–1.0 μm stage may be due in part to some hygroscopic growth of particles in that size range, because the ADI sizes particles at a fixed RH of 65%, while the MOUDI was operated at ambient dew point. A recent paper on PM density (McMurry et al. 2002) shows some particle growth at RH as low as 65%, with an average particle diameter growth factor of about 10–15%, based on measurements done in Atlanta, GA. It is thus conceivable that the middle ADI monitor stage is collecting a small fraction of PM below 0.45 μm, but this cannot adequately account for the outliers nor the substantially higher concentrations measured in that stage compared to the MOUDI. Enhanced nitrate volatilization from the particles collected by the MOUDI is the more likely explanation. Similar to the observations made for the 0.45–1.0 μm size range, the low correlations between ADI and MOUDI in the 0.10–0.45 μm size range may be due to the varying degrees of nitrate loss on the MOUDI stages with differing temperature and humidity conditions.

The geometric means of the ratios of the size-resolved ADI monitor and MOUDI nitrate measurements are shown in Table 1. Given that due to nitrate sampling artifacts the HEADS measures higher nitrate levels than the MOUDI (Figure 1a), and that the $PM_{2.5}$ ADI compares well with the HEADS data (Figure 1c), one would expect the size-fractionated stages of the ADI monitor to also measure more nitrate than the corresponding MOUDI stage. This is, in fact, the observed result with all three size range geometric mean ADI to MOUDI ratios above 1 (Table 1). The ratio for the 1.0–2.5 mm size range of 1.26 is less than the ratios for the other two size ranges. Pairwise comparison between the ADI and MOUDI concentrations for that size range revealed that this ratio is not significantly different than 1 ($p = 0.19$), and the absolute (as opposed to relative) differences between the MOUDI and ADI nitrate concentrations are rather small, as indicated by the results shown in Table 1. A possible reason that there is better ADI and MOUDI agreement in the larger size range is that some of the particulate nitrate in these larger particles exists as sodium nitrate, a nonvolatile species. Through single particle analysis, Liu et al. (2000) found that nitrate in the larger particles in Riverside is often associated with sodium nitrate. Kleeman and Cass (1998) present model predictions for Claremont that show sodium to be associated with larger particles in the form of sodium nitrate. The model predicts that sodium chloride particles from the ocean are converted entirely to sodium nitrate by the time they reach Claremont, and that they are associated with particles grater than 1.0 μm in diameter. Hughes et al. (2000) report that these model results agree with a more quantitative presentation of single particle measurements that clearly show more sodium nitrate particles in size ranges above 1.0 μm. Unfortunately, direct sodium measurements of the MOUDI samples are not available. However, if a portion of the nitrate in the larger size range of the ADI is in the form of nonvolatile sodium nitrate, this could explain the better agreement between MOUDI and ADI in this size fraction. (The higher ADI:MOUDI ratios for the two smaller size ranges, in which nitrate exists as labile ammonium nitrate, are more subject to variability caused by changing atmospheric conditions. The ADI concentrations are significantly higher than the MOUDI for the 0.45–1.0 μm range ($p = 0.05$), and they approach significance ($p = 0.14$) for the 0.1–.45 μm range. As mentioned above, a possible explanation for the lack of a larger or significant difference in measurements for the smallest size range is the presence of some nitrate in particles less than 0.1 μm in diameter which are not collected by the ADI monitor.

Comparison of the Experimental Data with Theoretical Predictions on Volatilization Losses

The observed nitrate losses from the MOUDI impactor stages, which depend on RH, temperature, and particle-phase nitrate concentration, can be compared to predicted sampling efficiencies based on the theory of Zhang and McMurry (1987). In order to determine the theoretical losses from the MOUDI stages, we have followed a similar process to that described by Chang et al. (2000).

The sampling efficiency for a given species η_s of any sampler can be expressed as follows:

$$\eta_s = 1 - \frac{M_e}{M_d}, \qquad [1]$$

where M_d is the particulate species mass delivered to the sampler and M_e is the mass evaporating from the deposited particles. The mass delivered to the sampler is expressed by the following equation:

$$M_d = Q\ C_m t \eta, \qquad [2]$$

where C_m is the actual aerosol mass concentration upstream of the sampler, η is the collection efficiency of the sampler, Q is the volumetric flow rate, and t is the sampling duration.

The rate of evaporative mass transfer from a deposit surface to the gas in a flowing air stream can be expressed as follows:

$$M = K\ A \Delta\rho, \qquad [3]$$

where K is a mass transfer coefficient, A is the surface area of the deposit, and $\Delta\rho$ is the difference in vapor concentration just above the surface of the deposit and that of the free airstream. According to the theory of Zhang and McMurry (1987), a lower limit for the sampling efficiency of impactor samplers can be calculated by the following equation:

$$\eta_s = \frac{1}{1 + \xi[S + (1 - S)/\delta]\frac{\rho_e}{C_m}}. \quad [4]$$

Here η_s is the sampling collection efficiency of the filter or impactor sampler, δ is a dimensionless factor defined as $\Delta P/(P_0 - \Delta P)$, ρ_e/C_m is the ratio of the equilibrium gas-phase concentration averaged over the sampling period to the measured particle concentration, and S is the average saturation ratio at the sampler inlet, which varies from 0 to 1 (0 corresponds to a denuded impactor). For the undenuded MOUDI, the gases are usually assumed to be at equilibrium concentrations, therefore S is reasonably close to 1.

For impactors, ξ is calculated by the following equation (Zhang and McMurry 1987):

$$\xi_i = \mathrm{Sc}^{-0.64}\,\mathrm{Re}^{-1/2}\frac{\Delta P}{\eta(P_0 - \Delta P)} \times \left\{1.5\left(1 - \frac{\rho_a U_0^2}{4\Delta P}\right) + 2.42\left[\left(\frac{r_e}{R}\right)^{1.14} - 1\right]\right\}. \quad [5]$$

Here Sc is Schmidt number, defined as the ratio of the air kinematic viscosity (ν) to the diffusivity of evaporating species (D); Re is Reynolds number based on jet diameter; η is collection efficiency for nonvolatile species; ρ_a is air density; U_0 is impactor jet velocity; r_e is radius of impactor deposit; and R is impactor jet radius. For the purposes of our theoretical calculations, Sc was taken equal to 1.1 and the ratio of r_e/R was assumed to be equal to 1.3, similar to the assumptions made by Chang et al. (2000). The calculations of the ξ values for each MOUDI stage are not particularly sensitive to the r_e/R ratio for values in the range of 1.2–1.7. Based on the previous work by Chang et al. (2000), the values of ξ were assumed to be 0.003 and 0.02 for the 0.32 and 0.1 μm MOUDI stages, respectively.

The original particulate nitrate size distribution (i.e., prior to volatilization), which is essential in calculating C_m in Equation (4), is unknown. We thus assumed that the ADI concentrations represent the actual (or true) nitrate concentrations, an argument that is further supported by the very good overall agreement between the total ADI and HEADS nitrate $PM_{2.5}$ concentrations.

The equilibrium concentrations of nitric acid and ammonia were estimated from the dissociation constant of ammonium nitrate K_d at temperature T (in Kelvin); the dissociation constant (in ppb^2) is given by the following equation (Chang et al. 2000):

$$\ln(K_d) = 118.87 - \frac{24084}{T} - 6.025\ln(T). \quad [6]$$

K_d is also dependent on RH when it exceeds 65% (i.e., the deliquescence point of ammonium nitrate). Since in our experiments this was rarely the case, corrections for RH were neglected. Since the dissociation constant applies to a pure solid or saturated solution, the determined gas phase nitric acid and ammonia concentrations represent an upper limit. Similar approaches have been followed in previous studies attempting to model the losses of nitrate from impactor and filter samplers (Hering and Cass 1999; Zhang and McMurry 1987; Chang et al. 1999).

The logarithmic dependence of the dissociation constant on temperature and humidity implies that temperature and RH need to be measured in short time intervals in order to accurately estimate the ammonium nitrate dissociation constant. Temperature and RH inside the trailer where the MOUDI was located were measured and recorded every 30 min in our experiments. As the time scales required for a substantial change in either temperature or RH are typically higher than 30 min, this sampling scheme allowed us to obtain (at least in theory) reasonably accurate estimates of the equilibrium nitric acid concentrations over sampling periods as long as 24 h.

Figures 3a and 3b show the theoretical and experimentally determined sampling efficiencies for particulate nitrate for the 0.10–0.45 and 0.45–1.0 μm size ranges, respectively. The experimentally determined sampling efficiency is defined as the ratio of the MOUDI to ADI nitrate concentration. As evident from the data plotted in Figures 3a and 3b, very good agreement between the theory and field sampling data was observed, particularly considering the assumptions made. Along with the curve corresponding to $S = 1$, the curve corresponding to $S = 0$ is included in both figures in order to show a theoretical lower limit for sampling efficiencies associated with evaporative losses during sampling. All of the experimental data points fall within the $S = 0$ and $S = 1$ curves. An additional explanation for the differences between theoretical and experimental sampling efficiencies may be related to possible losses of nitric acid in the inlet of the sampler as well as on the surface of the aluminum isokinetic sampling probes used to bring the air sample into the MOUDI which was located inside a trailer. John et al. (1988) showed that the aluminum inlet of dichotomous samplers, when clean, could be an effective denuder for nitric acid. It is thus possible that some nitric acid is lost in the aluminum sampling probes. A plot of the theoretical curve corresponding to $S = 0.80$ (i.e., assuming a nitric acid loss of 20%) shows that MOUDI data is roughly approximated by this curve.

It should be emphasized that the purpose of this study was not to provide validation to the theory of evaporative losses by Zhang and McMurry (1987) but to demonstrate that the MOUDI to ADI nitrate concentration ratios in general follow the trends that would be predicted from previously developed models. The obtained agreement, however, at least in qualitative terms, is remarkable, particularly considering the uncertainties in estimating correctly the gas phase nitric acid concentrations.

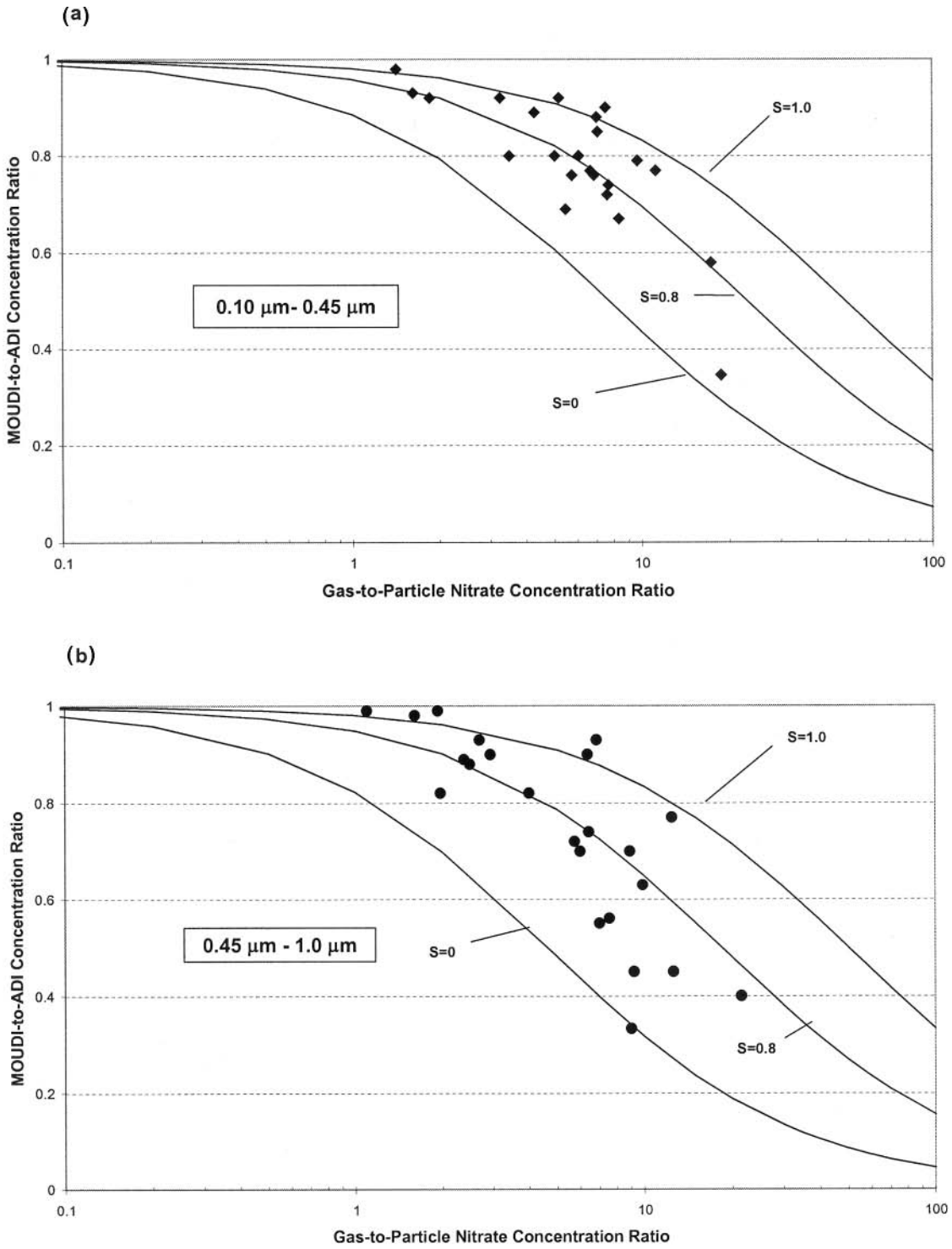

Figure 3. Differences in nitrate measurements between the ADI monitor and the MOUDI compared to theoretical nitrate sampling efficiencies for the size ranges (a) 0.10–0.45 μm and (b) 0.45–1.0 μm.

Continuous $PM_{2.5}$ Nitrate Size-Fractionated Ambient Data

These experiments were primarily designed to test the field performance of the ADI monitor under actual atmospheric conditions and particle concentrations. They were not intended to comprehensively explain size distributions and their diurnal and seasonal patterns in the Los Angeles basin. However, the following discussion provides some examples of the interesting patterns seen in the ambient continuous size-segregated particulate nitrate data over the six months of the study and also serves to demonstrate the utility of this type of data in trying to determine the sources, formation mechanisms, and transport of atmospheric particulate nitrate.

The contour plots in Figure 4 illustrate the diurnal and seasonal nitrate variations in each size range of the ADI monitor over the six months of the study. The 10-min nitrate data from

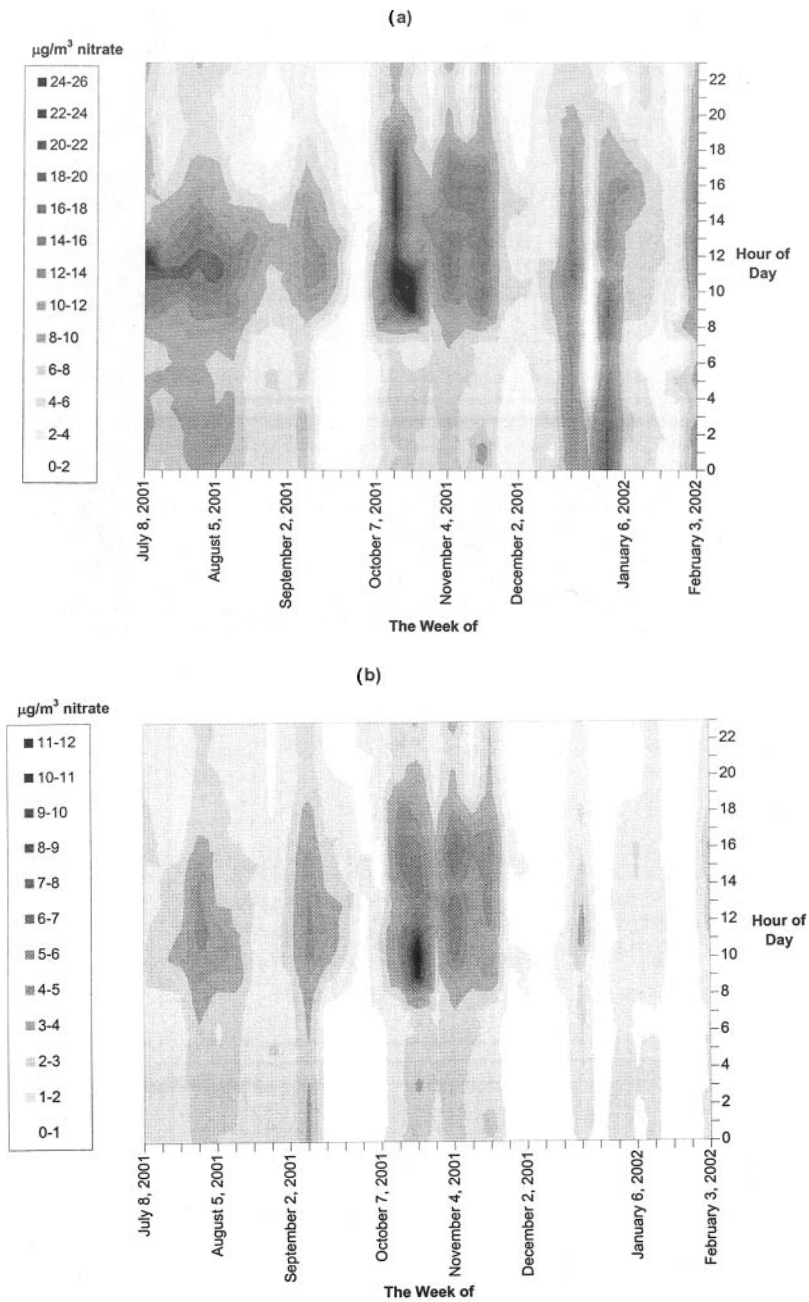

Figure 4. Seasonal and diurnal results of ambient nitrate measurements made by the ADI monitor for the following particle diameters: (a) Total $PM_{2.5}$, (b) 1.0–2.5 μm, (c) 0.45–1.0 μm, and (d) 0.10–0.45 μm. The plots combine data from Rubidoux (prior to September 15, 2001) and Claremont (after September 15, 2001). *(Continued)*

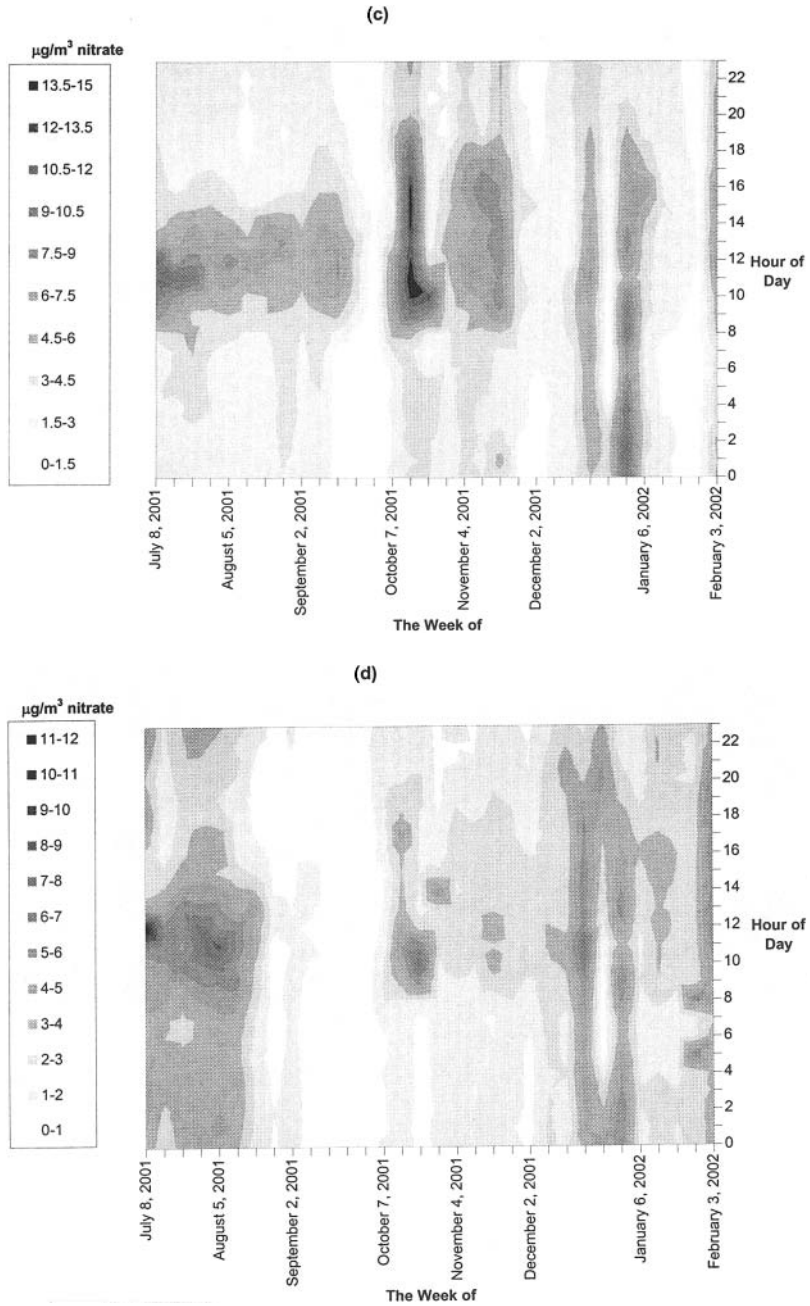

Figure 4. (Continued)

the ADI monitor was averaged to yield hourly nitrate concentrations for each size range. Then, composite weekly data were determined by calculating the average nitrate concentration of each hour of the day (0–23) across each day of the week (Sunday to Saturday). Thus, the vertical axis in the contour plots represents the hourly nitrate concentration over the course of the day, while seasonal variations can be read from left to right. Figure 4a represents the total $PM_{2.5}$ nitrate concentrations as measured by the sum of the three ADI monitor stages, and Figures 4b–4d display the corresponding results for each of the ADI monitor size ranges. The plots combine data from Rubidoux (prior to September 15, 2001) and Claremont (after September 15, 2001).

The plot of total $PM_{2.5}$ reveals midday particulate nitrate peaks over much of the six-month sampling time period. Daytime particulate nitrate peaks in the Los Angeles Basin are consistent with previous observations (Stolzenburg and Hering 2000; Liu et al. 2000) as well as model predictions (Russell et al. 1988). Early in the study, from July through mid-September, a single nitrate maximum is observed for most weeks between the hours of 10 a.m. and 1 p.m. The size-fractionated data in

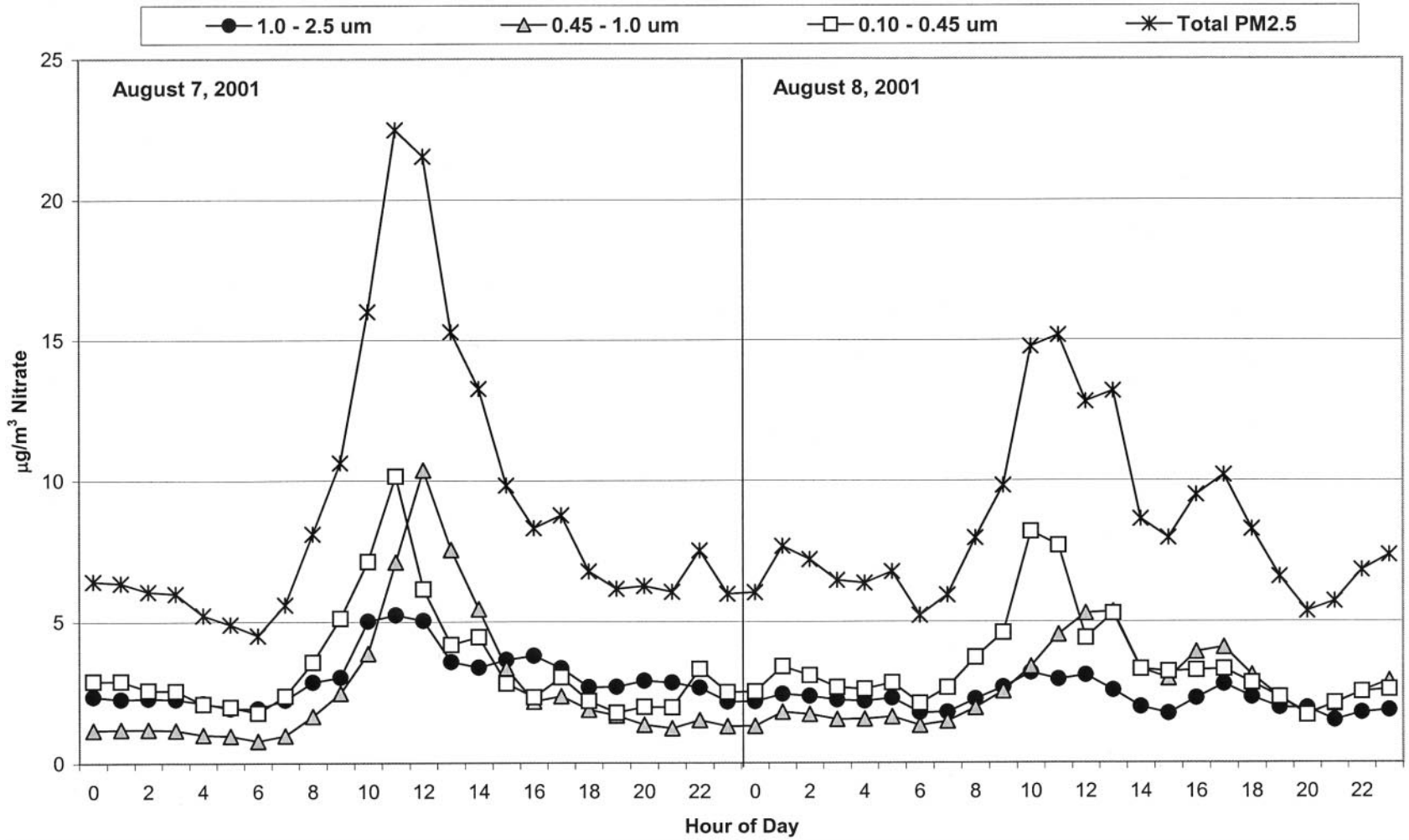

Figure 5. Size-fractionated hourly-averaged nitrate measurements from the ADI monitor for August 7–8, 2001 at Rubidoux, CA.

Figures 4b–4d illustrate that the smaller particle sizes are primarily responsible for these peaks, thereby suggesting a photochemical origin. A notable exception occurs during the second week of September, when the larger particles contribute more to the nitrate maximum, suggesting an aged aerosol due to local stagnation conditions or sodium nitrate from nitrate replacement on sea-salt particles. During that week of September, unusually high RHs by the standards of the Los Angeles Basin were observed. It is thus conceivable that some of the observed nitrate may be ammonium nitrate formed photochemically and grown to the supermicrometer range.

In some of the weeks in October and November of 2001, a second daily nitrate maximum is observed around 4 p.m. in addition to the midday peak. Size-resolved data indicate that these autumn maxima are caused by nitrate in the 0.45–1.0 μm particle range, whereas the late morning peak contains more of the smaller sized (i.e., 0.1–0.45 μm) particles. The latter peak may be due to agglomeration of the smaller particles produced during midday, enhanced also by the addition of aerosols originally emitted in upwind "source" areas of urban Los Angeles and advected to Claremont after aging in the atmosphere for several hours during their transport eastward to the inland valleys. The seasonal prevalence of these two phenomena and their associated impact on aerosol size distributions in the inland areas of the Los Angeles Basin has been demonstrated previously in modeling (Pandis et al. 1992) and experimental field studies (Kim et al. 2002; Singh et al. 2002).

In December, the nitrate peaks are less pronounced than the other months, with high particulate nitrate levels spread out over the entire day. This could be a result of the lower photochemical activity during this period. High nighttime and early morning concentrations are observed in the winter months, with most of the particulate nitrate found in the 0.1–0.45 μm range. This observation is also consistent with the dependence of the dissociation constant of ammonium nitrate on temperature and humidity (Wexler and Seinfeld 1991). Higher concentrations of nitrate in the particulate phase should be expected at lower temperatures and higher RH conditions, such as those typically prevailing in the wintertime evening and early morning hours.

Figure 5 provides an example of time-series hourly nitrate data for selected consecutive days in August 2001 from the Rubidoux sampling site. On the first day, August 7th, a single $PM_{2.5}$ nitrate maximum was observed between 10 a.m. and noon. The size-segregated data beneath the total $PM_{2.5}$ curve suggests that nitrate concentration peak initially contained a higher contribution from the smaller particles, and then in the next hour was primarily caused by particles in the middle size range. These results suggest rapid particle growth consistent with a photochemical episode and particle growth by agglomeration. The following day exhibits the same general pattern; nitrate associated with smaller particles contributes more to the total particulate nitrate earlier in the nitrate maximum. A second nitrate maximum occurred around 5:00 p.m. on the same day with a relatively large contribution from the largest particle size fraction.

Once again, a full account of particulate nitrate formation and transport in Los Angeles is beyond the scope of the current paper. Other factors such as temperature, relative humidity, precipitation, wind speeds, inversion heights, and air-parcel trajectories need to also be considered in such an effort. However, the size-fractionated and continuous nature of the data provided by the new ADI monitor can provide important clues as to the origin and formation mechanisms of atmospheric particulate nitrate.

SUMMARY AND CONCLUSIONS

The field evaluation of the new ADI size-fractionated ICVC continuous fine-particle nitrate monitor yielded good agreement with traditional time-integrated filter and impactor-based measurements. The $PM_{2.5}$ nitrate concentrations measured by the ADI monitor correlated well with HEADS measurements. Nitrate sampling artifacts in both of these measurement techniques are expected to be low. Comparisons of the ADI size-fractionated nitrate data to MOUDI impactor samples show less agreement due to volatilization of labile ammonium nitrate from the MOUDI impaction substrates. The ADI measured consistently more nitrate than the corresponding MOUDI stages, but to a lesser degree in the 1.0–2.5 μm size range, in which nitrate is more likely to exist as nonlabile sodium nitrate. The observed MOUDI nitrate losses are explained by existing theories of nitrate sampling efficiencies and can account for the general discrepancies between the ADI and MOUDI measurements.

The continuous nature of the data generated by the ADI monitor will provide valuable information on the spatial and temporal distribution of particulate nitrate in the atmosphere. The new capability to generate size-resolved data will now help to determine the sources and formation mechanisms of the atmospheric particulate nitrate as well.

REFERENCES

Appel, B. R., and Tokiwa, Y. (1983). Atmospheric Particulate Nitrate Sampling Errors Due to Reactions with Particulate and Gaseous Strong Acids, *Atmospheric Environment* 15:1087–1089.

Appel, B. R., Tokiwa, Y., Haik, M., and Kothny, E. L. (1984). Artifact Particulate Sulfate and Nitrate Formation on Filter Media, *Atmospheric Environment* 18:409.

Chang, M. C., Sioutas, C., Kim, S., Gong, H., and Linn, W. (2000). Reduction of Nitrate Losses from Filter and Impactor Samplers by Means of Concentration Enrichment, *Atmospheric Environment* 34:86–98.

Christoforou, C. S., Salmon, L. G., Hannigan, M. P., Solomon, P. A., and Cass, G. R. (2000). Trends in Fine Particle Concentration and Chemical Composition in Southern California, *Journal of the Air & Waste Management Association* 50(1):43–53.

Coutant, R. W. (1977). Effect of Environmental Variables on Collection of Atmospheric Sulfate, *Environmental Science and Technology* 11:873.

Dockery, D. W., Pope, C. A., Xu, X., Spengler, J. D., Ware, J. H., Ferris, B. G., and Speizer, F. E. (1993). An Association Between Air-Pollution and Mortality in 6 United-States Cities, *New England Journal of Medicine* 329(24):1753–1759.

Eatough, D. J., Benner, C. L., Lewis, L., Lamb, J. D., and Hansen, L. D. (1988). Annular Denuder and Filter Pack Collection of HNO_3(g), HNO_2(g), SO_2(g), and Particulate Phase Nitrate, Nitrite, and Sulfate in the Southwest Desert. WHITEX SPECIAL STUDY, 1987, Salt River Project.

Forrest, J., Tanner, R. L., Spandau, D., and Newman, L. (1980). Determination of Atmospheric Nitrate and Nitric Acid Employing a Diffusion Denuder with a Filter Pack, *Atmospheric Environment* 16:1473–1485.

Gordian, M. E., Ozkaynak, H., Xue, J. P., Morris, S. S., and Spengler, J. D. (1996). Particulate Air Pollution and Respiratory Disease in Anchorage, Alaska, *Environmental Health Perspectives* 104(3):290–297.

Hering, S., Eldering, A., and Seinfeld, J. H. (1997). Bimodal Character of Accumulation Mode Aerosol Mass Distributions in Southern California, *Atmospheric Environment* 31(1):1–11.

Hering, S. V., and Cass, G. R. (1999). The Magnitude of Bias in the Measurement of PM-2.5 Arising from Volatilization of Particulate Nitrate from Teflon Filters, *Journal of Air and Waste Management Association* 49(6):725–733.

Hughes, L. S., Allen, J. O., Bhave, P., Kleeman, M. J., Cass, G. R., Liu, D. Y., Fergenson, D. P., Morrical, B. D., and Prather, K. A. (2000). Evolution of Atmospheric Particles Along Trajectories Crossing the Los Angeles Basin, *Environmental Science and Technology* 43(15):3058–3068.

John, W., Wall, S. M., and Ondo, J. L. (1988). A New Method for Nitric Acid and Nitrate Aerosol Measurement using the Dichotomous Sampler, *Atmos. Environ.* 24A:2349–2359.

John, W., Wall, S. M., Ondo, J. L., and Winklmayr, W. (1990). Modes in the Size Distributions of Atmospheric Inorganic Aerosol, *Atmospheric Environment Part a-General Topics* 24(9):2349–2359.

Kim, S., Shi, S., Zhu, Y., Hinds, W. C., and Sioutas, C. (2002). Size Distribution, Diurnal and Seasonal Trends of Ultrafine Particles in Source and Receptor Sites of the Los Angeles Basin, *Journal of Air and Waste Management Association* 52:174–185.

Kleeman, M. J., and Cass, G. R. (1998). Source Contributions to the Size and Composition Distributions of Urban Particulate Air Pollution, *Atmos. Environ.* 32(16):2803–2816.

Koutrakis, P., Thompson, K. M., Wolfson, J. M., Spengler, J. D., Keeler, J., and Slater, J. (1992). Determination of Aerosol Strong Acidity Losses Due to Interactions of Collected Particles—Results from Laboratory and Field Studies, *Atmospheric Environment Part a-General Topics* 26(6):987–995.

Liu, D. Y., Prather, K. A., and Hering, S. V. (2000). Variations in the Size and Chemical Composition of Nitrate-Containing Particles in Riverside, CA, *Aerosol Science and Technology* 33:71–86.

McMurry, P. H., Wang, X., Park, K., and Ehara, K. (2002). The Relationship Between Mass and Mobility for Atmospheric Particles: A New Technique for Measuring Particle Density, *Aerosol Science and Technology* 36(2):227–238.

Mozurkewich, M. (1993). The Dissociation-Constant of Ammonium Nitrate and Its Dependence on Temperature, Relative Humidity and Particle-Size, *Atmospheric Environment Part a-General Topics* 27(2):261–270.

Pandis, S. N., Harley, R. A., Cass, G. R., and Seinfeld, J.H. (1992). Secondary Organic Aerosol Formation and Transport, *Atmospheric Environment Part a-General Topics* 26(13):2269–2282.

Russell, G. R., McCue, K. F., and Cass, G. R. (1988). Mathematical Modeling of the Formation of Nitrogen-Containing Air Pollutants. 1. Evaluation of an Eulerian Photochemical Model, *Environmental Science & Technology* 22(3):263–271.

Schwartz, J., and Dockery, D. W. (1992). Particulate Air-Pollution and Daily Mortality in Steubenville, Ohio, *American Journal of Epidemiology* 135(1):12–19.

Singh, M., Jaques, P., and Sioutas, C. (2002). Particle-Bound Metals in Source and Receptor Sites of the Los Angeles Basin, *Atmospheric Environment* 36:1675–1680.

Smith, J. P., Grosjean, D., and Pitts, J. N. (1978). Observation of Significant Losses of Particulate Nitrate and Ammonium from High Volume Glass Fiber Filters and Samples Stored at Room Temperature, *Journal of the Air Pollution Control Association* 28:929.

Stelson, A. W., and Seinfeld, J. H. (1982). Relative Humidity and Temperature Dependence of the Ammonium Nitrate Dissociation Constant, *Atmospheric Environment* 16:983–992.

Stolzenburg, M. R., Dutcher, D., Kirby, B., Kreisberg, N., and Hering, S. V. (2002). Automated Measurement of the Size Distribution of Airborne Particulate Nitrate, *Aerosol Science & Technology* in press.

Stolzenburg, M. R., and Hering, S. V. (2000). Method for the Automated Measurement of Fine Particle Nitrate in the Atmosphere, *Environmental Science & Technology* 34(5):907–914.

Tang, I. N. (1980). Deliquescence Properties and Particle Size Change of Hygroscopic, Aerosols, in *Generation of Aerosols*, K. Willeke ed., Ann Arbor Science, Ann Arbor, MI, pp. 153–168.

Vedal, S. (1997). Ambient Particles and Health: Lines that Divide, *Journal of the Air & Waste Management Association* 47(5):551–581.

Wang, H. C., and John, W. (1988). Characteristics of the Berner Impactor for sampling inorganic ions, *Aerosol Science and Technology* 8:157–172.

Wexler, A. S., and Seinfeld, J. H. (1991). 2nd-Generation Inorganic Aerosol Model, *Atmospheric Environment Part a-General Topics* 25(12):2731–2748.

Witz, S., Eden, R. W., Wadley, M. W., Dunwoody, C., Papa, R. P., and Torre, K. J. (1990). Rapid Loss of Particulate Nitrate, Chloride and Ammonium on Quartz Fiber Filters During Storage, *Journal of the Air & Waste Management Association* 40(1):53–61.

Zhang, X., and McMurray, P. H. (1987). Theoretical Analysis of Evaporative Losses from Impactor and Filter Deposits, *Atmospheric Environment* 21:1779–1789.